[CANCER RESEARCH 61, 6892–6898, September 15, 2001]

Neuroblastic and Schwannian Stromal Cells of Neuroblastoma Are Derived from a Tumoral Progenitor Cell[1]

Jaume Mora, Nai-Kong V. Cheung, Gloria Juan, Peter Illei, Irene Cheung, Muzaffar Akram, Susan Chi, Marc Ladanyi, Carlos Cordon-Cardo, and William L. Gerald[2]

Departments of Pediatrics [J. M., N-K. V. C., I. C., S. C.] and Pathology [J. M., G. J., P. I., M. A., M. L., C. C-C., W. L. G.], Memorial Sloan-Kettering Cancer Center, New York, New York 10021

ABSTRACT

The coexistence of neuroblastic and Schwannian stromal (SS) cells in differentiating neuroblastoma (NB), and derivation of Schwannian-like cells from neuroblastic clones *in vitro*, were accepted previously as evidence of a common pluripotent tumor stem line. This paradigm was challenged when SS cells were suggested to be reactive in nature. The advent of microdissection techniques, PCR-based allelic analysis, and *in situ* fluorescent cytometry made possible the analysis of pure cell populations in fresh surgical specimens, allowing unequivocal determination of clonal origins of various cell subtypes. To overcome the complexity and heterogeneity of three-dimensional tissue structure, we used: (*a*) Laser-Capture Microdissection to obtain histologically homogeneous cell subtype populations for allelotype analysis at chromosomes 1p36, 11q23, 14q32, and 17q and study of *MYCN* copy number; (*b*) multiparametric analysis by Laser-Scanning Cytometry of morphology, DNA content, and immunophenotype of intact cells from touch imprints; and (*c*) bicolor fluorescence *in situ* hybridization on touch imprints from manually microdissected neuroblast and stroma-rich areas. Histologically distinct SS and neuroblastic cells isolated by Laser-Capture Microdissection had the same genetic composition in 27 of 28 NB analyzed by allelic imbalance and gene copy number. In all 20 cases studied by Laser-Scanning Cytometry, SS cells identified by morphology and S-100 immunostaining had identical DNA content and GD2-staining pattern as their neuroblastic counterparts. In 7 cases, fluorescence *in situ* hybridization demonstrated the same chromosomal makeup for SS and neuroblastic cells. These results provide unequivocal evidence that neuroblastic and SS cells in NB are derived from genetically identical neoplastic cells and support the classical paradigm that NB arises from tumoral cells capable of development along multiple lineages.

INTRODUCTION

NB[3] is a pediatric cancer that arises from precursor cells of the peripheral sympathetic nervous system. Biologically, it has a wide range of behavior, including spontaneous regression/involution, spontaneous or induced maturation/differentiation, and aggressive proliferation. Spontaneous or induced differentiation of NB could recapitulate neural crest development with the formation of cells along multiple lineages (1, 2). In fact, histologically mature NB consists of two main cell populations, neuroblastic/ganglionic cells and non-neuronal stromal cells, including Schwann, perineurial, and satellite cells.

It is well established that the presence of SS in NB is age- and stage-related. Typically, infants with stage 4 tumors (International Neuroblastoma Staging system; Ref. 3), as well as aggressively proliferating tumors (International Neuroblastoma Staging system stage 4), are histologically SS poor (4, 5). Abundant SS is frequently seen in LR NB tumors with maturation potential and correlates closely with favorable genetic findings, *i.e.*, triploidy (6, 7). The origin of the stromal component and whether the presence of stroma is a cause or a consequence of the maturation potential of tumor cells is not yet fully established.

The coexistence of neuroblastic and SS cells in maturing NB and the appearance of Schwannian-appearing cells in NB cell cultures led to the hypothesis that NBs originate from pluripotent neural-crest cells. *In vitro*, three related cell types exist: the S-type with characteristics of immature Schwannian, glial, or melanocytic cells; the N-type with neuronal characteristics, and the I-type neural crest stem cells (8, 9). An alternative hypothesis was suggested by Ambros *et al.* (10) in 1996. They reported that SS cells in maturing NB lacked the genetic anomalies found in the neuroblastic cells and hypothesized that the SS cells in NB were reactive in nature and have been recruited from the surrounding nonneoplastic tissues. On the basis of known interactions between neuroblasts and their supporting stroma, they proposed that the recruited normal SS cells may be producing antiproliferative- and differentiation-inducing factors leading to maturation of neoplastic cells.

However, other studies of advanced stage disease suggest otherwise, *e.g.*, stromal-like cells derived from bone marrow metastases after temporary passages *in vitro* share some of the genetic abnormalities with the neuroblastic counterpart, suggesting a common tumoral origin (11). In addition, genetic analysis of homogeneous populations of cells isolated by LCM from diploid stage 4 NB showed identical genetic alterations in both SS and neuroblastic components (12).

In this study, we analyzed the clonal origin of the neuroblastic and non-neuronal cell subtypes (identified by morphology as SS) from fresh surgical specimens. To overcome the complexity and heterogeneity of three-dimensional structure of tissues, three different approaches were taken: (*a*) LCM was used to obtain histologically homogeneous cell subtype populations for analysis of 1p36, 11q, 14q, and 17q allelotype and *MYCN* copy number; (*b*) LSC was used to provide multiparametric information about morphology, DNA content, and immunophenotype of intact cells from touch imprints; and (*c*) bicolor FISH in cases where touch imprints of the two cell types could be manually microdissected.

MATERIALS AND METHODS

Tumor Tissues and Clinical Data. Forty frozen tumor specimens each with >75% tumor cell content, obtained from 17 patients with stage 4 NB patients and 23 patients with LR NB, were studied. Tumors (28) were used for LCM analysis, 20 for the LSC experiments, and 7 for FISH analysis. Human tissues were used for biological studies, according to the guidelines of the institutional review board. Clinical and biological characteristics for all cases are summarized in Table 1.

LCM and Genotype Analysis. LCM (13) was performed using a PixCell I system (Arcturus Engineering, Mountain View, CA) with 30–60 μm laser spot size applying default to full-strength pulse power (40–100 W) and the

Received 4/24/01; accepted 7/16/01.

The costs of publication of this article were defrayed in part by the payment of page charges. This article must therefore be hereby marked *advertisement* in accordance with 18 U.S.C. Section 1734 solely to indicate this fact.

[1] Supported in part by the American Society of Clinical Oncology Young Investigator Award 2000 (to J. M.), the JP's Wish Fund, the Katie-Find-a-Cure Fund, the Katie Hoch Foundation, and the Pediatric Cancer Foundation of New York.

[2] To whom requests for reprints should be addressed, at Department of Pathology, Memorial Sloan-Kettering Cancer Center, 1275 York Avenue, New York, NY 10021. Phone: (212) 639-5905; Fax: (212) 639-4559; E-mail: geraldw@mskcc.org.

[3] The abbreviations used are: NB, neuroblastoma; SS, Schwannian stromal; LR, local regional; LCM, Laser-Capture Microdissection; LSC, Laser-Scanning Cytometry; FISH, fluorescence *in situ* hybridization; PI, propidium iodide; AI, allelic imbalance; LOH, loss of heterozygosity; FCM, flow cytometry.

Table 1 *Clinical and biological characteristics for all tumors analyzed*

No.	Tumor	Tissue histology	*MYCN* status	1p36 status	FCM DNA index	Age (yrs)	Stage (INSS)	Therapy	Outcome
1	1140-Dx[a]	NB	NotAmpl	AI	1.4	2.0	1	Sx	A
2	2022-Dx	NB	NotAmpl	Intact	1	8.0	1	CCG	A
3	949-Dx	GNB	NotAmpl	AI	1.2	0.3	2	Sx	A
4	2052-rel	GNB	NotAmpl	Intact	1.5	6.0	2	CCG	A
5	2019-Dx	NB	NotAmpl	Intact	1	0.1	2	Sx	A
6	755-Dx	GNB	NotAmpl	LOH	1	0.4	2	N6	A
7	1367-Dx	NB	Ampl	LOH	1	1.0	2	Sx	A
8	2140-Dx	NB	NotAmpl	AI		6.0	2	CT	A
9	2174-Dx	GNB	NotAmpl	AI		2.0	2	Sx	A
10	1163-Dx	NB	NotAmpl	AI	1.5	1.7	3	N7	D
11	1637-Dx	GNB	NotAmpl	Intact	1	6.0	3	N7	D
12	2130-Dx	NB	NotAmpl	AI	1.5	2.0	3	Sx	A
13	1564-Dx	NB	Ampl	LOH	1	1.8	3	N7	D
14	1571-Dx	NB	Ampl	Intact	1	3.0	3	N7	D
15	2132-Dx	NB	NotAmpl	Intact	1.4	1.0	3	Sx	A
16	2147-Dx	GNB	NotAmpl	LOH	1	2.0	3	Sx	A
17	1915-PC	GNB	NotAmpl	AI	1.4	3.0	3	POG	A
18	2001-PC	GNB	NotAmpl	Intact	1	2.0	3	CT	A
19	1641-PC	GNB	NotAmpl	AI	1.5	3.0	3	POG	A
20	1905-PC	GNB	NotAmpl	Intact	1.4	0.8	3	CCG	A
21	1649-Dx	GN	NotAmpl	Intact		12.0	GN	Sx	A
22	1021-Dx	GN	NotAmpl	Intact		3.0	GN	Sx	A
23	916-Dx	GN	NotAmpl	Intact		3.0	GN	Sx	A
24	2123-PC	NB	NotAmpl/Ampl[b]	Intact	1.4	0.6	4	N6	A
25	849-Dx	NB		MM		9.0	4	N6	A
26	1631-Dx	NB	NotAmpl	Intact		5.5	4	N7	A
27	1381-Dx	NB	Ampl	LOH	1	0.8	4	N7	D
28	1396-Dx	NB	NotAmpl	Intact	1	0.9	4	N7	A
29	1940-Dx[c]	NB	NotAmpl	Intact	1.2	1.1	4	Sx	A
30	1824-Dx	NB	NotAmpl	Intact		29.0	4	N7	A
31	1090-2nd	NB		Intact	1	2.9	4	N6	D
32	1822-2nd	NB	NotAmpl	Intact		14.0	4	N7	D
33	1914-2nd	NB	NotAmpl	LOH	1	3.6	4	N7	A
34	1843-2nd	NB	NotAmpl	LOH		8.0	4	N7	A
35	1850-2nd	NB	NotAmpl	LOH		5.0	4	N7	A
36	1893-2nd	NB	NotAmpl	Intact	1.9	0.7	4	N7	A
37	1296-2nd	NB	NotAmpl	MM		4.2	4	N7	A
38	1436-rel	NB	NotAmpl	LOH		8.0	4	N7	D
39	1599-rel	NB	NotAmpl	Intact	1	4.0	4	N7	A
40	1785-rel	NB	NotAmpl	LOH		1.6	4	N7	D

[a] Dx, at diagnosis; PC, after induction chemotherapy; rel, at relapse; NB, NB with <50% stroma; GNB, ganglioneuroblastoma with >50% stroma; GN, ganglioneuroma- or stroma-dominant tumor; NotAmpl, not amplified; Ampl, amplified; MM, microsatellite mutation; Sx, surgery alone; CCG and POG, multimodality protocols from Children's Cancer Group or Pediatric Oncology Group; N6 and N7, multimodality protocols from Memorial Sloan-Kettering Cancer Center; INSS, international neuroblastoma classification system; A, alive; D, dead.

[b] Multiple tumoral populations of cells detected by FISH using the LSI-MYCN DNA probe, one with highly amplified *MYCN* and the other with three to five copies.

[c] This patient has a stage 4 according to the INSS but biologically and clinically has been managed as stage 4S with no cytotoxic therapy.

extreme strength of the pulse width (50–100 ms). Neuroblastic cell samples contained 1000–2000 cells, and SS samples were composed of 500-1000 cells. DNA and RNA from tumor, normal, and LCM samples were extracted according to standard procedures (14).

Allelic analysis of samples was performed using polymorphic microsatellite markers D1S548, D1S1592, D1S2826, D1S552, and D1S511 for chromosome arm 1p36; D11S1982, D11S488, D11S1294, D11S1302, and D11S1366 for chromosome arm 11q23; and D14S544, D14S120, D14S302, D14S140, D14S119, and D14S129 for chromosome arm 14q32. To investigate chromosome gain at 17q, we followed the microsatellite-based approach of Janoueix-Lerosey *et al.* (15) using D17S796, D17S938, D17S1176, and D17S786 at chromosome 17p13 and D17S693, D17S916, D17S674, D17S1304, and D17S668 at chromosome 17q25. Alleles were measured using an Applied Biosystems model 310 automated fluorescent DNA sequencer (Applied Biosystems, Foster City, CA) with Genescan software (16). LOH was determined by comparison of the allelic ratio between the normal and tumor or LCM specimen in heterozygous samples as described previously (17).

Relative quantitation of *MYCN* and the endogenous control β-actin was performed by real-time quantitative PCR using an Applied Biosystems Prism 7700 Sequence detection system. The primers and probe were designed using the applications-based primer design software primer express (Applied Biosystems). PCR protocol was performed according to the manufacturer guidelines. Every PCR run included a five-point standard derived from serial dilutions of NB cell line LAN-1 DNA to generate a standard curve for *MYCN* and β-actin, plus a no-template control. For each unknown test sample, the amount of *MYCN* and endogenous β-actin was determined from the respective standard curve. Dividing the *MYCN* level by the β-actin level resulted in a normalized *MYCN* value.

Immunocytochemical Detection of GD2 and S-100. Touch imprints were obtained after 10 consecutive previous touch preparations from frozen tumor blocks to eliminate previously cut cells. Immunocytochemical detection was performed following standard methods (18, 19). The slides were fixed in 80% ice-cold ethanol at −20°C for ≤24 h, washed twice with PBS containing 1% BSA and 0.1% sodium azide PBS-BSA, and blocked for 30 min with 5% normal goat serum in PBS. Then cells were incubated overnight in the dark at 4°C with 100 μl of PBS-BSA containing 2 μg/ml mouse anti-GD2 monoclonal antibody (3F8), a recognized marker for NB cells (20), 2 μg/ml anti-S-100 monoclonal antibody (BioGenex Laboratories, San Ramon, CA), or 2 μg/ml mouse anti-IgG as a negative isotype control. Slides were then washed in PBS-BSA and incubated with 100 μl of secondary antibody conjugated to FITC (Dako, Carpinteria, CA) for 30 min in the dark at room temperature. Finally, the cells were stained in PBS containing 5 μg/ml PI and 100 μg/ml RNase A for 30 min at room temperature. The slides were then mounted under coverslips in PBS for analysis by LSC.

The specificity of the immunofluorescence staining was confirmed by a titration of the monoclonal antibodies GD2 and S-100. Normal lymph node (negative control), tumor samples, and one NB cell line (SK-N-ER; positive control) were used. Five dilutions were tested ranging from 0.2 μg/ml to 3.3 μg/ml. Two μg/ml was the selected concentration based on the lack of staining in lymph nodes and the highest fluorescence intensity in the positive control (tumor samples). Concentrations as high as 3.3 μg/ml, however, did not show

increased nonspecific staining in lymph nodes or improved staining in the tumor samples.

LSC. Cytometric measurements were performed using a laser scanning cytometer (LSC 101; Compucyte Corp., Cambridge, MA) as described previously (21). The excitation wavelength was 488 nm. Green (FITC) and red (PI) fluorescences were measured by separate photomultipliers within 530 ± 20 nm and 600 ± 20 nm spectral ranges, respectively. An additional light source provided transmitted illumination, which was used to visualize the cells through an eyepiece or a CCD camera (21, 22). At least 3000 cells were analyzed per sample.

FISH. Bicolor FISH studies were performed on touch imprints obtained from manual microdissection of stromal and neuroblastic-rich areas using probe mixtures of the directly labeled centromere-specific alphoid sequences for chromosomes 1 and 17 (CEP1 and CEP17; Vysis, Downer's Grove, IL) and a mixture of two probes localized to sub-regions of 17q25 (525L23 and 497H17 RPC11 human bacterial artificial chromosome). One μg of each DNA probe was directly labeled using a nick translation kit (Vysis) according to the manufacturer's instructions. The labeled DNA was then coprecipitated for annealing purposes with 2 μg of Cot-1 DNA (sonicated total human DNA). The telomeric location of the probes was confirmed by hybridizing to metaphase spreads of normal human lymphocytes in a bicolor assay with directly labeled centromere 17-specific alphoid sequence (CEP17; Vysis). FISH was performed according to standard protocols and previously published studies (23). Images were prepared using the Applied Image Analysis System (Applied Imaging, Pittsburgh, PA). The number of hybridization signals for each probe was assessed in a minimum of 200 interphase nuclei with strong and well-delineated signals. As controls, normal peripheral blood lymphocytes were simultaneously hybridized with these probes.

RESULTS

Allelotype and *MYCN* Analysis in LCM Specimens. Neuroblastic and SS components of the tumor were identified by morphology and isolated by LCM (Fig. 2). LCM samples adequate for allelic analysis were obtained in 28 (12 LR NB and 16 stage 4) samples. Twenty-seven of the 28 cases (96%) showed identical genetic features in the whole tumor and individual cellular components. Table 2 summarizes the results of the allelotype analysis for all of the subpopulations obtained by LCM. Figs. 1 and 2 show examples of AI and LOH electropherograms obtained for the microdissected neuroblastic and SS specimens from tumors 2140, 1381, 1940, and 1163.

Among the 12 LR NB tumors analyzed, 11 had genetic abnormalities that could be detected in all of the samples analyzed. Five tumors showed AI secondary to chromosome 1 triploidy (Figs. 1 and 2) concordant with the near triploid DNA index found by FCM (Table 1) or FISH (see below). One tumor (tumor 1564, Table 2) showed gain of material at chromosome 17q, and 5 tumors had 1p36 LOH that was present in the SS and neuroblastic LCM samples and the whole tumor. Samples from 1 tumor (tumor 1905) did not show any allelic abnormality for any locus studied. Among the 16 stage 4 tumors, 10 had identical allelic abnormalities detected in all tissue samples, including 5 tumors with 1p36 LOH, 2 with 1p36 microsatellite mutations, 2 with 11q23 LOH, and 1 with gain of material at chromosome arm 17q. Five tumors had no detectable allelic alterations at the loci studied in any of the samples analyzed. In 1 tumor (tumor 1436, Table 2), the 1p36 LOH found in the whole tumor and neuroblastic counterpart specimens was not detected in the SS component, suggesting the presence of normal stromal cells.

In 1 *MYCN*-amplified tumor (tumor 1381), we were able to obtain enough sample for comparison of *MYCN* copy number between neuroblastic and SS cell subtypes by quantitative PCR. On the basis of eight replicative quantitations, the patient's normal tissue control *MYCN* copy number was 1.3 ± 1.8, whereas the LCM neuroblast sample had 360 ± 297, and the LCM SS sample had 106 ± 157 *MYCN* copies.

Cytometric Analysis. LSC was used to evaluate the DNA ploidy *in vivo* on each cell subtype. SS cells were identified by morphology and independently by indirect immunofluorescence with the S-100 monoclonal antibody. The tumor-specific anti-GD2 monoclonal antibody 3F8 was used to mark tumor clones (20). 3F8 binds strongly to NB, whereas it is unreactive with most normal human tissues, including blood and marrow (20, 24). LSC analysis was performed in 19 LR tumors because abnormalities of DNA index are common in LR NB

Table 2 *Allelotype summary*

No.	LR NB	Whole tumor Genescan data	LCM neuroblast cells Genescan data	LCM Schwannian stroma Genescan data
1	1140-Dx[a]	1p36 and 17q AI	1p36 and 17q AI	1p36 and 17q AI
2	949-Dx	1p36 AI	1p36 AI	1p36 AI
3	1163-Dx	1p36 AI	1p36 AI	1p36 AI
4	1905-PC	Intact 1p36 and 17q	Intact 1p36 and 17q	Intact 1p36 and 17q
5	1641-PC	1p36 AI	1p36 AI	1p36 AI
6	1564-Dx	17q AI	17q AI	17q AI
7	755-Dx	1p36 LOH	1p36 LOH	1p36 LOH
8	1367-Dx	1p36 LOH	1p36 LOH	1p36 LOH
9	2140-Dx	1p36 AI	1p36 AI	1p36 AI
10	1649-Dx			1p36 LOH
11	1021-Dx			1p36 LOH
12	916-Dx			1p36 LOH
Stage 4				
1	849-Dx	1p36 MM	1p36 MM	1p36 MM
2	1631-Dx	11q LOH	11q LOH	11q LOH
3	1381-Dx	1p36 LOH	1p36 LOH	1p36 LOH
4	1396-Dx	11q LOH	11q LOH	11q LOH
5	1940-Dx	1p; 11q; 14q; 17q intact	1p; 11q; 14q; 17q intact	1p; 11q; 14q; 17q intact
6	1824-Dx	1p; 11q; 14q; 17q intact	1p; 11q; 14q; 17q intact	1p; 11q; 14q; 17q intact
7	1090-2nd	1p; 11q; 14q; 17q intact		1p; 11q; 14q; 17q intact
8	1822-2nd	1p; 11q; 14q; 17q intact		1p; 11q; 14q; 17q intact
9	1914-2nd	1p36 LOH		1p36 LOH
10	1843-2nd	1p36 LOH		1p36 LOH
11	1850-2nd	1p36 LOH	1p36 LOH	1p36 LOH
12	1893-2nd	1p; 14q intact; 17q GAIN		1p; 14q intact; 17q GAIN
13	1296-2nd	1p36 MM		1p36 MM
14	1436-rel	1p36 LOH	1p36 LOH	1p36 intact
15	1599-rel	1p; 11q; 14q intact		1p; 11q; 14q intact
16	1785-rel	1p36 LOH		1p36 LOH

[a] Dx, at diagnosis; PC, after induction chemotherapy; rel, at relapse; MM, microsatellite mutation.

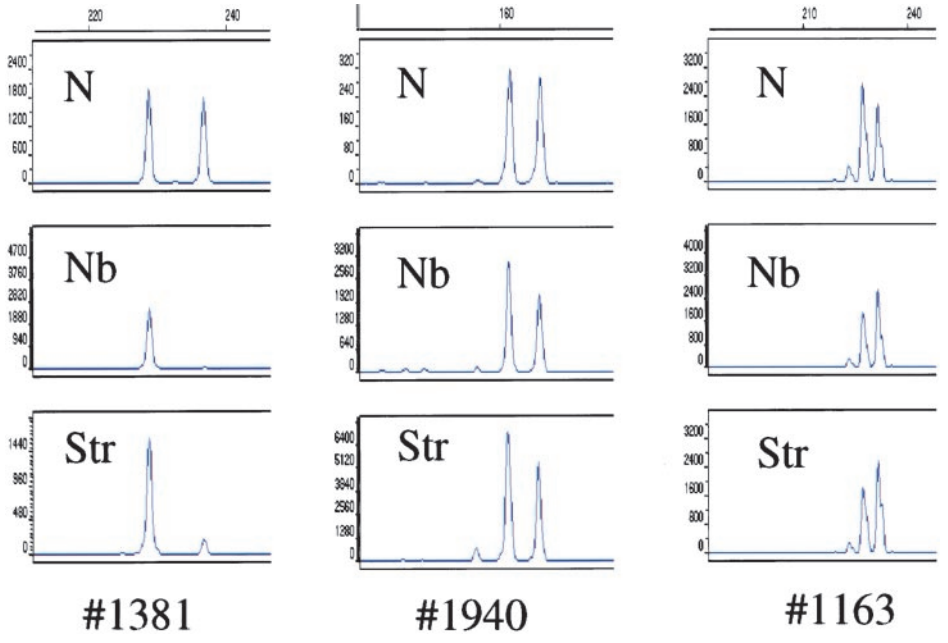

Fig. 1. Representative electropherograms showing examples of retention of heterozygosity (*center*), LOH (*left panel*), and AI secondary to triploidy (*right panel*) for the LCM neuroblastic (*Nb*) and Schwannian-Stroma (*Str*). *X* axis, allele bp size; *Y* axis, relative immunofluorescence intensity.

and 1 stage 4 tumor with multiple clones identified by FISH for *MYCN* (Tumor #2123, Table 1). The results are summarized in Table 3.

The first set of experiments was done by multiparametric analysis of DNA content (PI) and anti-GD2 monoclonal antibody 3F8 (FITC) immunofluorescence. The ploidy peaks obtained in the LSC analysis matched the histogram patterns obtained with parallel samples by FCM (data not shown). One tumor had a predominant hyperploid population of GD2-positive cells (tumor 1641, Table 3), and 10 tumors had a single diploid clonal peak of GD2-positive cells (tumors 1564, 755, 1367, 1571, 2022, 2052, 2019, 1021, 2140, and 2174, Table 3). Seven tumors (tumors 949, 1163, 2130, 2123, 1649, 916, and 2132, Table 2) showed both diploid and hyperploid peaks that were positive by GD2 staining, suggesting that in these cases, both the diploid as well as the hyperploid clones were of tumoral origin (Fig. 2). Two tumors (tumors 1140 and 1905, Table 3) had diploid and hyperploid clones, but only the hyperploid peak was GD2 positive, suggesting that the small diploid population was predominantly normal cells, although down-regulation of GD2 expression in tumoral-derived stroma could not be ruled out. We could identify spindle-shaped (non-neuroblastic) stromal cells by morphology in all tumors with hyperploid peaks among the hyperploid GD2+ cells using the relocation feature of LSC and H&E staining (Fig. 3).

LSC experiments were repeated using S-100 expression to identify SS cells. Results are summarized in Table 3. Nine tumors had S-100-positive cells in >30% of the cells examined. In 6 of these tumors (tumors 1140, 1905, 1641, 2123, 916, and 2132), S-100-positive cells were detected in the hyperploid clones, all of which were also positive for GD2 by the previous analysis (Fig. 4). Three of these tumors

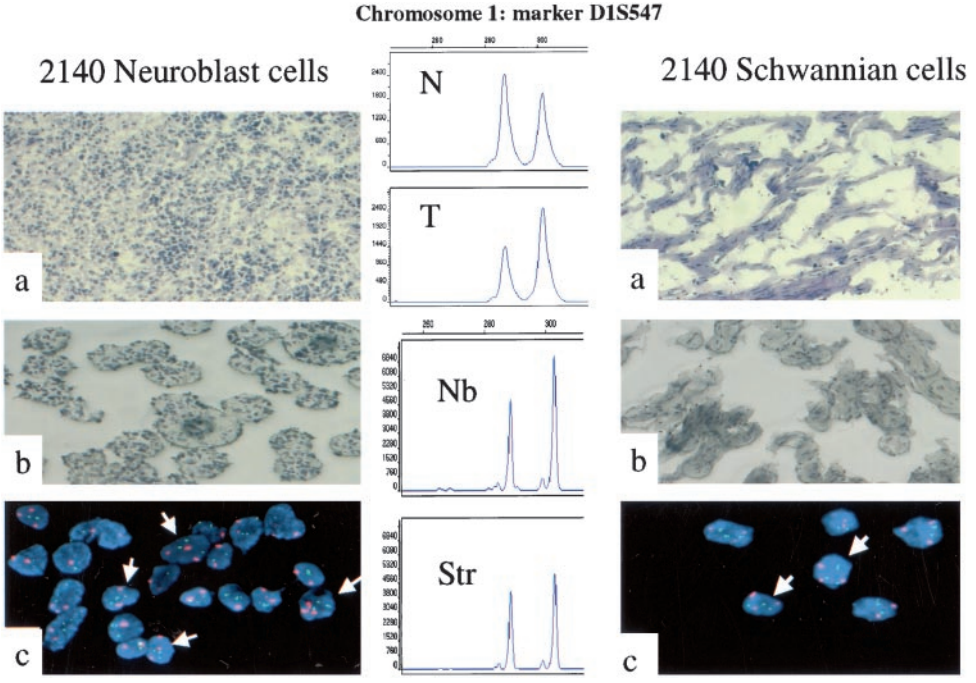

Fig. 2. Allelotype and FISH analysis of the LR tumor 2140 show triploidy of chromosomes 1 and 17 for both cell subtypes. *a*, photomicrographs showing histology of neuroblastic-rich region (*left*) and SS-rich area (*right*) of tumor 2140 before LCM. *b*, neuroblastic cells (*left*) and SS cells (*right*) obtained after LCM and subsequently used for allelotype analysis. *Center panels*, the AI detected by allelotype analysis secondary to the triploidy for microsatellite marker D1S547 at chromosome 1q: *N*, normal (blood); *T*, whole tumor; *Nb*, LCM neuroblasts; and *Str*, LCM SS cells. *c*, FISH analysis using chromosome 1 and 17 centromeric probes (*red* and *green*, respectively) of touch imprints obtained after manual microdissection of the neuroblastic and SS-rich areas of tumor 2140 showing triploidy for both chromosomes (three *green* and *red* signals).

Table 3 *Multiparametric analysis of DNA content and GD2 or S-100 expression by LSC*[a]

No.	Tumors	Histology	Ploidy peaks	GD2+ staining	S-100+ staining
1	1649-Dx[b]	GN	D+A	D+A	
2	1021-Dx	GN	D	D	D
3	916-Dx	GN	D+A	D+A	D+A
4	949-Dx	GNB	D+A	D+A	Ne
5	1905-PC	GNB	D+A	A	D+A
6	1641-PC	GNB	A	A	A
7	755-Dx	GNB	D	D	Ne
8	2052-Rel	GNB	D	D	D
9	2174-Dx	GNB	D	D	Ne
10	1140-Dx	NB	D+A	A	A
11	1163-Dx	NB	D+A	D+A	Ne
12	1564-Dx	NB	D	D	Ne
13	1367-Dx	NB	D	D	Ne
14	1571-Dx	NB	D	D	Ne
15	2022-Dx	NB	D	D	Ne
16	2019-Dx	NB	D	D	Ne
17	2130-Dx	NB	D+A	D+A	Ne
18	2123-PC	NB	D+A	D+A	D+A
19	2140-Dx	NB	D	D	D

[a] GD2 and S-100 staining by LSC was considered positive when >30% of cells analyzed stained positive, whereas cases with <30% positive cells were considered nonevaluable.

[b] Dx, at diagnosis; PC, after induction chemotherapy; rel, at relapse; NB, NB tumor with <50% stroma; GNB, ganglioneuroblastoma tumor with >50% stroma; GN, ganglioneuroma- or stroma-dominant tumor; D, diploid; A, aneuploid; D+A, both diploid and aneuploid peaks are positive; Ne, nonevaluable.

(tumors 1140, 1641, and 916) showed AI or LOH when the Genescan analysis of the SS LCM specimen for that case was performed (Table 2). Nine tumors had <30% S-100-positive cells and were considered nonevaluable.

FISH Analysis. Touch imprints from manually microdissected stroma-rich and neuroblastic areas were obtained in 7 tumors (tumors 2140, 2147, 1637, 1915, 2052, 2001, and 1641). Three signals for both chromosome 1 and 17 were obtained in both the neuroblasts and SS cells for the triploid tumors 1915 and 2140 (Table 1; Fig. 1). Tumor 1637 showed two signals for chromosome 1 and 17 centromeric probes but three signals for chromosome 17q25 probe in both the neuroblasts and SS cells, indicating a selective gain of 17q25 genetic material. The rest of the tumors studied had two signals for chromosome 1 and 17 in both the neuroblasts and SS cells in concordance with their diploid status.

DISCUSSION

One major limitation of using human tumors for clonal studies is the difficulty in partitioning complex mixture of different cell types in the three-dimensional structure of tissues. To overcome these technical difficulties, we combined fluorescent cytometry and image and genetic analysis with advanced microdissection laboratory technology. LCM allows the procurement of homogeneous cell populations from heterogeneous tissue (13). Using LCM samples, we analyzed both neuroblasts and SS cells in isolation. Our results show unequivocally that both cell components of individual tumors are genotypically identical and tumor derived. In addition, we used LSC, a microscope-based cytometer that provides the unique advantages of image analysis and cytometry measurements on intact single cells (21). Using LSC, we could show that stroma cells identified by morphology and S-100 immunostaining showed the same GD2 immunoreactivity and DNA index as corresponding neuroblasts from the same tumor.

Because FISH can convincingly mark chromosome gains or losses in individual cells, the presence of aberrant signals is often accepted as proof of tumoral origin. Ambros *et al.* (10) showed that Schwannian cells from NB with maturing histological features lacked the chromosome 1p36 triploidy found in the neuroblastic cells, leading to the hypothesis that the Schwann cells were normal cells recruited into the tumor during the maturation process. However, the absence of evidence cannot be equated as the evidence of absence given the heterogeneity inherent in most human tumors. Furthermore, FISH analysis on cut paraffin sections as used by Ambros *et al.* are sometimes difficult to interpret because of the high degree of cellular heterogeneity and randomly sectioned nuclei, requiring statistical estimates of DNA content. This may explain the differences between our findings and previous studies (10). In contrast, FISH carried out on touch imprints of separate neuroblastic and stromal areas of tumors avoids many of these pitfalls. Unfortunately, the intimate admixture of tumor and stroma cell subtypes in most human tumors precluded the use of this technique for most cases. In all evaluable cases, FISH analysis of touch imprints unequivocally detected identical chromosomal makeup for neuroblast and corresponding SS cells

LR NB is characterized clinically by a lack of metastatic potential,

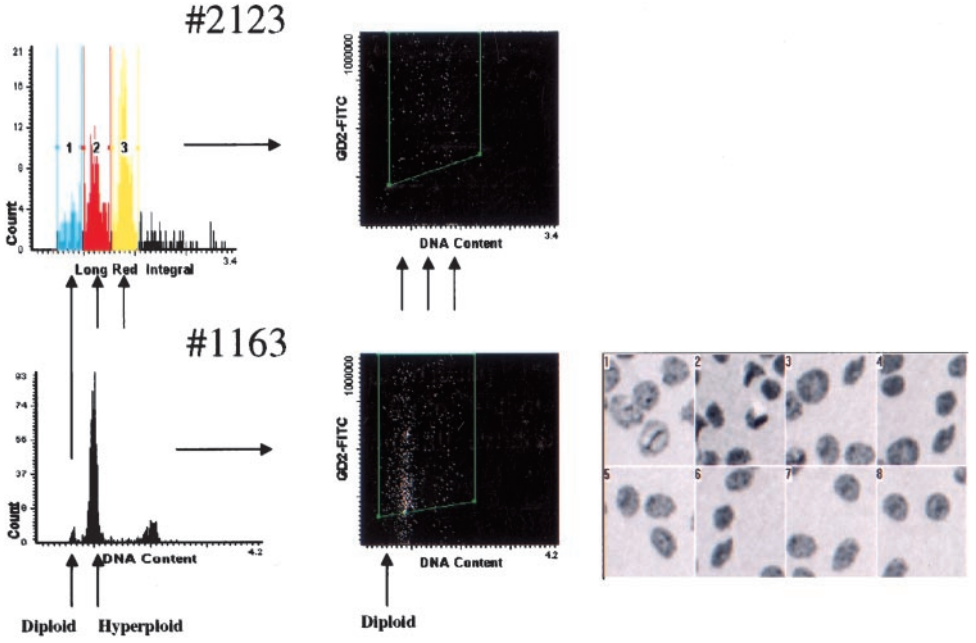

Fig. 3. DNA content and cytology of GD2-positive cells in NB. *Left panels*, DNA content distributions of two tumor samples. The percentage of cells in each peak was estimated after staining of cellular DNA with PI and fluorescence measurement by LSC. *Center panels*, bivariate distributions (scatterplots) of GD2-immunofluorescence *versus* DNA content of the same sample. The analytical gate was set as described in "Materials and Methods." *Arrows*, the ploidy peaks. Tumor 2123 shows three discrete ploidy peaks, one diploid and two hyperploid, all GD2 positive. Tumor 1163 shows a small diploid and a prominent hyperploid peak, all GD2 positive. After LSC measurement, cells that highly expressed GD2 were selected for viewing. Characteristic small-round cell morphology for neuroblastic cells was confirmed, and a gallery of digital images was created (*right panel*).

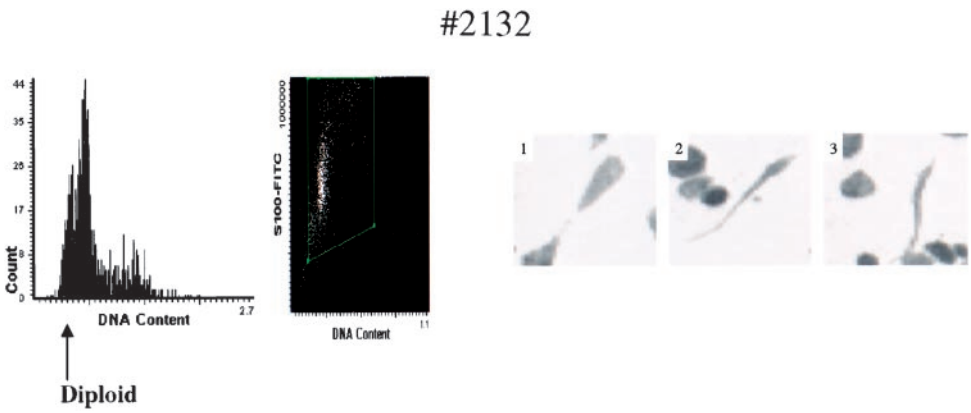

Fig. 4. Multiparametric analysis by LSC of S-100 expression, DNA content, and nuclear cell morphology. DNA content distribution of tumor sample 2132 shows two discrete ploidy peaks: one diploid and one hyperploid (*left panel*). Bivariate distribution of S-100 immunofluorescence *versus* DNA content of the same sample shows S-100-positive, hyperploid cells (*center panel*). Cells that highly expressed S-100 were gated and selected for viewing (*right panel*). Cells with spindle morphology (*SS*) were detected in the fields.

a propensity for maturation (25), and various degrees of differentiation at the histological level. In one previous study, we found that near triploid DNA index was the best predictive marker of progression-free survival in LR NB independent of the presence or absence of significant stromal component (7). The data provided in this study show that most cases of LR NB have a triploid DNA index in the neuroblastic as well as in the stroma compartments.

In contrast, NB tumors with aggressive proliferation and metastatic behavior (stage 4) are characterized by diploid DNA index, structural chromosomal aberrations, and *MYCN* gene amplification (26). Histologically, they are mostly stroma poor (5). After cytotoxic therapy, a significant percentage of stage 4 cases are left with or acquire a differentiated stroma. In this group of tumors, the presence of abundant stroma had no survival significance in our series (data not shown), as well as in other reports (27). Our results show that both neuroblasts and stromal cells have the same genetic composition and suggest that current cytotoxic therapies may either induce the maturation of neuroblastic cells to undergo non-neuronal differentiation or fail to kill the stromal elements. In this context, the *in vitro* observation that S-type cells can trans-differentiate into N-type cells under certain pressures takes particular significance (28). If this phenomenon occurs *in vivo*, the late relapses commonly seen in stage 4 cases postchemotherapy could be attributable to viable non-neuroblastic stromal cells. In this particular group of highly malignant NB tumors, new therapies addressing specifically the stromal compartment of tumor cells might be important. The observation that S-type cells may also be resistant to complement mediated cytotoxicity because of their surface expression of decay-accelerating factor (CD55), CD59, and CD45 additionally underscores the limitations of current antibody-based immunotherapy strategies (29).

An interesting finding from our LSC analysis is that the widely accepted assumption in flow-cytometry, that the presence of a diploid peak in a hyperploid tumor reflects nontumoral origin (30), may not always be true. The presence of small diploid GD2-positive clonal peaks in cases with predominant hyperploid clonal populations suggests that both are tumor derived. This and previous studies describing tumors with evolution of two clonal tumoral ploidy populations (31) suggest that the triploid clones may have arisen from diploid clones that had undergone endoduplication and subsequent triploidization as proposed by some investigators (32, 33).

In conclusion, our results provide evidence that neuroblasts and stromal cells in NB are of neoplastic origin and that the presence of stroma is a consequence (not a cause) of the maturation potential of tumor cells. These data support the hypothesis that NB arises from a tumoral neural crest cell capable of development along multiple lineages.

ACKNOWLEDGMENTS

We thank Drs. Robert A. Ross, Barbara A. Spengler, and June Biedler for helpful discussions and review of the manuscript and Lishi Chen for his technical assistance.

REFERENCES

1. Tsokos, M., Scarpa, S., Ross, R. A., and Triche, T. J. Differentiation of human neuroblastoma recapitulates neural crest development. Study of morphology, neurotransmitter enzymes, and extracellular matrix proteins. Am. J. Pathol., *128:* 484–496, 1987.
2. Ross, R. A., Spengler, B. A., and Biedler, J. L. Coordinate morphological and biochemical interconversion of human neuroblastoma cells. J. Natl. Cancer. Inst. (Bethesda), *71:* 741–747, 1983.
3. Brodeur, G. M., Pritchard, J., Berthold, F., Carlsen, N. L., Castel, V., Castelberry, R. P., De Bernardi, B., Evans, A. E., Favrot, M., Hedborg, F., Kaneko, M., Kemshead, J., Lampert, F., Lee, R. E. J., Look, T., Pearson, A. D. J., Philip, T., Roald, B., Sawada, T., Seeger, R. C., Tsuchida, Y., and Voute, P. A. Revisions of the international criteria for neuroblastoma diagnosis, staging, and response to treatment. J. Clin. Oncol., *11:* 1466–1477, 1993.
4. Shimada, H., Ambros, I. M., Dehner, L. P., Hata, J. I., Joshi, V. V., and Roald, B. Terminology and morphologic criteria of neuroblastic tumors. Cancer (Phila.), *86:* 349–363, 1999.
5. Shimada, H., Ambros, I. M., Dehner, L. P., Hata, J., Joshi, V. V., Roald, B., Stram, D. O., Gerbing, R. B., Lukens, J. N., Matthay, K. K., and Castleberry, R. P. The International Neuroblastoma Pathology Classification (the Shimada System). Cancer (Phila.), *86:* 364–372, 1999.
6. Ambros, P. F., Ambros, I. M., Strehl, S., Baur, S., Luegmayr, A., Kovar, H., Ladenstein, R., Fink, F. M., Horcher, E., and Printz, G. Regression and progression in neuroblastoma. Does genetics predict tumour behaviour? Eur. J. Cancer, *31A:* 510–515, 1995.
7. Mora, J., Gerald, W., Chen, L., Qin, J., and Cheung, N. K. V. Survival analysis of clinical, pathologic and genetic features in neuroblastoma presenting as local-regional disease. Cancer (Phila.), *91:* 435–442, 2001.
8. Biedler, J. L., Helson, L., and Spengler, B. A. Morphology and growth, tumorigenicity, and cytogenetics of human neuroblastoma cells in culture. Cancer Res., *33:* 2643–2652, 1973.
9. Ross, R. A., Spengler, B. A., Domenech, C., Porubcin, M., Rettig, W. J., and Biedler, J. L. Human neuroblastoma I-type cells are malignant neural crest stem cells. Cell Growth Differ., *6:* 449–456, 1995.
10. Ambros, I. M., Zellner, A., Roald, B., Amann, G., Ladenstein, R., Printz, D., Gadner, H., and Ambros, P. F. Role of ploidy, chromosome 1p, and Schwann cells in the maturation of neuroblastoma. N. Engl. J. Med., *334:* 1505–1511, 1996.
11. Valent, A., Benard, J., Venuat, A. M., Silva, J., Duverger, A., Duarte, N., Hartmann, O., Spengler, B. A., and Bernheim, A. Phenotypic diversity of human neuroblastoma studied in three IGR cell line models derived from bone marrow metastases. Cancer Genet. Cytogenet., *112:* 124–129, 1999.
12. Mora, J., Akram, M., Cheung, N. K., Chen, L., and Gerald, W. L. Laser-capture microdissected schwannian and neuroblastic cells in stage 4 neuroblastomas have the same genetic alterations. Med. Pediatr. Oncol., *35:* 534–537, 2000.
13. Simone, N. L., Bonner, R. F., Gillespie, J. W., Emmert-Buck, M. R., and Liotta, L. A. Laser-capture microdissection: opening the microscopic frontier to molecular analysis. Trends Genet., *14:* 272–276, 1998.
14. Maniatis, T., Fritsch, E. F., and Sambrock, J. (eds.). Molecular Cloning: A Laboratory Manual. Cold Spring Harbor, NY: Cold Spring Harbor Laboratory; 1989.
15. Janoueix-Lerosey, I., Penther, D., Thioux, M., de Cremoux, P., Derre, J., Ambros, P., Vielh, P., Benard, J., Aurias, A., and Delattre, O. Molecular analysis of chromosome arm 17q gain in neuroblastoma. Genes Chromosomes Cancer, *28:* 276–284, 2000.
16. Mora, J., Cheung, N. K., Kushner, B. H., LaQuaglia, M. P., Kramer, K., Fazzari, M., Heller, G., Chen, L., and Gerald, W. L. Clinical categories of neuroblastoma are

associated with different Patterns of loss of heterozygosity on chromosome arm 1p. J. Mol. Diag., *2:* 37–46, 2000.
17. Cawkwell, L., Bell, S. M., Lewis, F. A., Dixon, M. F., Taylor, G. R., and Quirke, P. Rapid detection of allele loss in colorectal tumours using microsatellites and fluorescent DNA technology. Br. J. Cancer, *67:* 1262–1267, 1993.
18. Juan, G., and Darzynkiewicz, Z. Cell cycle analysis by flow and laser-scaning cytometry. *In:* J. E. Celis (ed.), Cell Biology: A Laboratory Handbook, Ed. 2, pp. 255–268. San Diego, CA: Academic Press, Inc., 1998.
19. Juan, G., and Cordon-Cardo, C. Intranuclear compartimentalization of cyclin E during the cell cycle: disruption of the nucleoplasm-nucleolar shuttling of cyclin E in bladder cancer. Cancer Res., *61:* 1220–1226, 2001.
20. Cheung, N. K., Saarinen, U. M., Neely, J. E., Landmeier, B., Donovan, D., and Coccia, P. F. Monoclonal antibodies to a glycolipid antigen on human neuroblastoma cells. Cancer Res., *45:* 2642–2649, 1985.
21. Kamentsky, L. A., Burger, D. E., Gershman, R. J., Kamentsky, L. D., and Luther, E. Slide-base laser scanning cytometry. Acta Cytol., *41:* 123–143, 1997.
22. Deptala, A., Bedner, E., Gorczyca, W., and Darzynkiewicz, Z. Activation of nuclear factor κB (NF-κB) assayed by laser-scanning cytometry (LSC). Cytometry, *33:* 376–382, 1998.
23. Illei, P., Feiner, H., Yin, H., Chan, W., Symmans, F., and Perle, M. A. Interphase cytogenetic study of chromosomes 7, 18 and X in tissue scrapes of proliferative fibrocystic disease and ductal carcinoma *in situ* of the breast. Breast J, *4:* 252–257, 1998.
24. Saito, M., Yu, R. K., and Cheung, N. K. V. Ganglioside GD2 specificity of monoclonal antibodies to human neuroblastoma cell. Biochem. Biophys. Res. Commun., *127:* 1–4, 1985.
25. Kushner, B. H., Cheung, N. K., LaQuaglia, M. P., Ambros, P. F., Ambros, I. M., Bonilla, M. A., Gerald, W. L., Ladanyi, M., Gilbert, F., Rosenfield, N. S., and Yeh, S. D. Survival from locally invasive or widespread neuroblastoma without cytotoxic therapy. J. Clin. Oncol., *14:* 373–381, 1996.
26. Maris, J. M., and Matthay, K. K. Molecular biology of neuroblastoma. J. Clin. Oncol., *17:* 2264–2279, 1999.
27. Kubota, M., Suita, S., Tajiri, T., Shono, K., and Fujii, Y. Analysis of the prognostic factors relating to better clinical outcome in ganglioneuroblastoma. J. Pediatr. Surg., *35:* 92–95, 2000.
28. Biedler, J. L., Soengler, B. A., Chang, T., and Ross, R. A. Transdifferentiation of human neuroblastoma cells results in coordinate loss of neuronal and malignant properties. *In:* A. E. Evans, G. J. D'Angio, A. G. Knudson, and R. C. Seeger (eds.), Advances in Neuroblastoma Research, Ed. 2, pp. 265–276. New York: Alan R. Liss, Inc., 1988.
29. Chen, S., Caragine, T., Cheung, N. K. V., and Tomlinson, S. Surface antigen expression and complement susceptibility of differentiated neuroblastoma clones. Am. J. Pathol., *156:* 1085–1091, 2000.
30. Hedley, D. W. Flow cytometry using paraffin-embedded tissue: five years on. Cytometry, *10:* 229–241, 1989.
31. Mora, J., Cheung, N. K. V., and Gerald, W. Genetic heterogeneity and clonal evolution in neuroblastoma. Br. J. Cancer, *85:* 182–189, 2001.
32. Kaneko, Y., and Knudson, A. G. Mechanism and relevance of ploidy in neuroblastoma. Genes Chromosomes Cancer, *29:* 89–95, 2000.
33. Taylor, S. R., Blatt, J., Costantino, J. P., Roederer, M., and Murphy, R. F. Flow cytometric DNA analysis of neuroblastoma and ganglioneuroma. A 10-year retrospective study. Cancer (Phila.), *62:* 749–754, 1988.

Neuroblastic and Schwannian Stromal Cells of Neuroblastoma Are Derived from a Tumoral Progenitor Cell

Jaume Mora, Nai-Kong V. Cheung, Gloria Juan, et al.

Cancer Res 2001;61:6892-6898.